Synthetic Routes to Fe_2S_2, Fe_3S_4, Fe_4S_4, and Fe_6S_9 Clusters from the Common Precursor $[Fe(SC_2H_5)_4]^{2-}$: Structures and Properties of $[Fe_3S_4(SR)_4]^{3-}$ and $[Fe_6S_9(SC_2H_5)_2]^{4-}$, Examples of the Newest Types of Fe–S–SR Clusters

Karl S. Hagen, Alan D. Watson, and R. H. Holm*

Contribution from the Department of Chemistry, Harvard University, Cambridge, Massachusetts 02138. *Received November 4, 1982*

Abstract: The strongly reducing, tetrahedral Fe(II) complex $[Fe(SEt)_4]^{2-}$ (**1**) serves as a versatile precursor to Fe–S–SR clusters. With 1.0–1.5 equiv of elemental sulfur **1** reacts to form three types of clusters, $[Fe_2S_2(SEt)_4]^{2-}$ (**2**), $[Fe_3S_4(SEt)_4]^{3-}$ (**3**), and $[Fe_6S_9(SEt)_2]^{4-}$ (**4**). In acetonitrile at ~25 °C **1** and 1.0 equiv of sulfur afford the $(Me_3NCH_2Ph)^+$ salt of **2** in 80% yield. This compound is converted quantitatively to previously known $[Fe_4S_4(SEt)_4]^{2-}$ (**5**) in acetonitrile at 80 °C. In acetone at ~25 °C **1** and 1.4 equiv of sulfur give $[Fe_3S_4(SEt)_4]^{3-}$ (66%) as its Et_4N^+ salt. At 60 °C in acetonitrile $(Et_4N)_3$(**3**) is converted to $(Et_4N)_4$(**4**) (32%), which can also be obtained in higher yield from **1** and 1.5 equiv of sulfur in acetonitrile at 85 °C. Clusters **2** and **5** are examples of structural types already established. $(Et_4N)_3[Fe_3S_4(SPh)_4]$, obtained from **3** by ligand substitution with benzenethiol, crystallizes in orthorhombic space group $Pna2_1$ with a = 36.748 (4) Å, b = 9.114 (2) Å, c = 17.427 (4) Å, and Z = 4. With 7657 unique data ($I > 3\sigma(I)$) the structure was refined to R = 3.9%. The Fe_3S_8 portion of the anion approaches D_{2d} symmetry and consists of two tetrahedral FeS_4 units corner-linked by a central Fe atom, also in a tetrahedral site. The two outer Fe atoms are each terminally coordinated by two thiolates. The $[Fe_3(\mu_2\text{-}S)_4]^+$ core unit, a new element in the structural chemistry of Fe–S clusters, has a mean Fe···Fe separation of 2.714 Å and other dimensions similar to the $[Fe_2S_2]^{2+}$ cores of $[Fe_2S_2(SR)_4]^{2-}$. $(Et_4N)_4$(**4**)·4MeCN crystallizes in triclinic space group $P\bar{1}$ with a = 11.537 (3) Å, b = 11.706 (3) Å, c = 28.45 (1) Å, α = 98.14 (3)°, β = 81.80 (3)°, γ = 110.91 (2)°, and Z = 2. The structure was refined to R = 4.1% on the basis of 4202 unique data ($I > 3\sigma(I)$). The anion has the same structure as that previously demonstrated for $[Fe_6S_9(S\text{-}t\text{-}Bu)_2]^{4-}$, with a $[Fe_6(\mu_2\text{-}S)_6(\mu_3\text{-}S)_2(\mu_4\text{-}S)]^{2-}$ core containing three types of bridging sulfur atoms and closely approaching C_{2v} symmetry. Certain spectroscopic, magnetic, and reactivity properties of clusters **2**–**5** are described. The latter property includes the trinuclear–tetranuclear conversion $[Fe_3S_4(SEt)_4]^{3-} \rightarrow [Fe_4S_4(SEt)_4]^{2-}$ effected in acetonitrile with $FeCl_2$ alone or in the presence of NaSEt. The complexes $[Fe_3S_4(SR)_4]^{3-}$ (EPR g value ≅ 4.2) are the first synthetic trinuclear clusters of the $Fe_3(S^{2-})_x$ type ($x \geq 3$). Their linear core structure is apparently different from the arrangement of the Fe_3S_x site in *D. gigas* ferredoxin II ($g \cong 2.01$ in the oxidized form), a recent EXAFS analysis of which indicates similar Fe–Fe distances (~2.7 Å).

Introduction

The extensive development of the chemistry of iron–sulfide–thiolate systems over the last 10 years has resulted in the isolation and detailed characterization of three structural types of complexes.[1-3] These are mononuclear tetrahedral $[Fe(SR)_4]^{2-,1-}$, binuclear $[Fe_2S_2(SR)_4]^{2-}$ containing the planar $[Fe_2(\mu_2\text{-}S)_2]^{2+}$ core, and tetranuclear $[Fe_4S_4(SR)_4]^{3-,2-}$ containing the cubane-type $[Fe_4(\mu_3\text{-}S)_4]^{1+,2+}$ cores. Such species have found widespread use as synthetic analogues of the redox sites in iron–sulfur proteins. Our recent demonstration[4] of reactions 1–5 in Scheme I of Figure 1 has provided the first definitions of reaction sequences leading to the formation of Fe–S–SR clusters. The scheme features high-yield reactions between elemental sulfur and Fe(II)–thiolates, adamantane-like $[Fe_4(SPh)_{10}]^{2-}$[5] in reaction 2 and $[Fe(SPh)_4]^{2-}$[6] in reaction 4, and stepwise elaboration of the tetranuclear cluster by reactions 3–5. No other cluster species were identified in the course of the derivation of Scheme I.

Despite the preeminence of Fe_2S_2 and Fe_4S_4 clusters since the first example, $[Fe_4S_4(SCH_2Ph)_4]^{2-}$, was synthesized in 1972,[7] there has been no evident reason why stable, isolable Fe–S–SR clusters should be confined to these two types. The first indication of the existence of another structural type was afforded by crystallographic identification of the $Fe_3(\mu_3\text{-}S)_3$ cycle in *A. vinelandii* ferredoxin I.[8] Trinuclear units have since been detected in a number of other Fe–S proteins. That in *D. gigas* ferredoxin II[9] is apparently different in structural detail from the cyclic structure in *A. vinelandii* ferredoxin I. The 3-Fe units in aconitase[10] and *D. gigas* ferredoxin II[11,12] can be converted to Fe_4S_4 clusters by reaction with Fe(II) and Fe(II) + sulfide, respectively. In an effort commenced several years ago our first realization of a new cluster type was $[Fe_6S_9(S\text{-}t\text{-}Bu)_2]^{4-}$,[13,14] including the remarkable $[Fe_6(\mu_2\text{-}S)_6(\mu_3\text{-}S)_2(\mu_4\text{-}S)]^{2-}$ core. Subsequent to our initial report[13] the corresponding benzylthiolato cluster, prepared by a different method, was described by Henkel et al.[15] The trinuclear complex $[Fe_3S(S_2\text{-}o\text{-}xyl)_3]^{2-}$, having a pyramidal $[Fe_3(\mu_3\text{-}S)]^{4+}$ central unit, has recently been synthesized in this laboratory.[16] A ring-sub-

(1) Berg, J. M.; Holm, R. H. In "Iron-Sulfur Proteins"; Vol. 4 of "Metal Ions in Biology"; Spiro, T. G., Ed.; Wiley-Interscience: New York, 1982; Chapter 1.
(2) Holm, R. H.; Ibers, J. A. In "Iron-Sulfur Proteins"; Vol. 3 of "Metal Ions in Biology"; Lovenberg, W., Ed.; Academic Press: New York, 1977; Chapter 7.
(3) Holm, R. H. *Acc. Chem. Res.* **1977**, *10*, 427.
(4) Hagen, K. S.; Reynolds, J. G.; Holm, R. H. *J. Am. Chem. Soc.* **1981**, *103*, 4054.
(5) Hagen, K. S.; Berg, J. M.; Holm, R. H. *Inorg. Chim. Acta* **1980**, *45*, L17. Hagen, K. S.; Stephan, D. W.; Holm, R. H. *Inorg. Chem.* **1982**, *21*, 3928.
(6) Coucouvanis, D.; Swenson, D.; Baenziger, N. C.; Murphy, C.; Holah, D. G.; Sfarnas, N.; Simopoulos, A.; Kostikas, A. *J. Am. Chem. Soc.* **1981**, *103*, 3350.
(7) Herskovitz, T.; Averill, B. A.; Holm, R. H.; Ibers, J. A.; Phillips, W. D.; Weiher, J. F. *Proc. Natl. Acad. Sci. U.S.A.* **1972**, *69*, 2437.
(8) Ghosh, D.; Furey, W., Jr.; O'Donnell, S.; Stout, C. D. *J. Biol. Chem.* **1981**, *256*, 4185. Ghosh, D.; Furey, W., Jr.; Robbins, A. H.; Stout, C. D. *J. Mol. Biol.* **1982**, *158*, 73.
(9) Antonio, M. R.; Averill, B. A.; Moura, I.; Moura, J. J. G.; Orme-Johnson, W. H.; Teo, B. K.; Xavier, A. V. *J. Biol. Chem.* **1982**, *257*, 6646.
(10) Kent, T. A.; Dreyer, J.-L.; Kennedy, M. C.; Huynh, B. H.; Emptage, M. H.; Beinert, H.; Münck, E. *Proc. Natl. Acad. Sci. U.S.A.* **1982**, *79*, 1096.
(11) Kent, T. A.; Moura, I.; Moura, J. J. G.; Lipscomb, J. D.; Huynh, B. H.; LeGall, J.; Xavier, A. V.; Münck, E. *FEBS Lett.* **1982**, *138*, 55.
(12) Moura, J. J. G.; Moura, I.; Kent, T. A.; Lipscomb, J. D.; Huynh, B. H.; LeGall, J.; Xavier, A. V.; Münck, E. *J. Biol. Chem.* **1982**, *257*, 6259.
(13) Christou, G.; Holm, R. H.; Sabat, M.; Ibers, J. A. *J. Am. Chem. Soc.* **1981**, *103*, 6269.
(14) Christou, G.; Sabat, M.; Ibers, J. A.; Holm, R. H. *Inorg. Chem.* **1982**, *21*, 3518.
(15) Henkel, G.; Strasdeit, H.; Krebs, B. *Angew. Chem., Int. Ed. Engl.* **1982**, *21*, 201; *Angew. Chem. Suppl.* **1982**, 489.

0002-7863/83/1505-3905$01.50/0

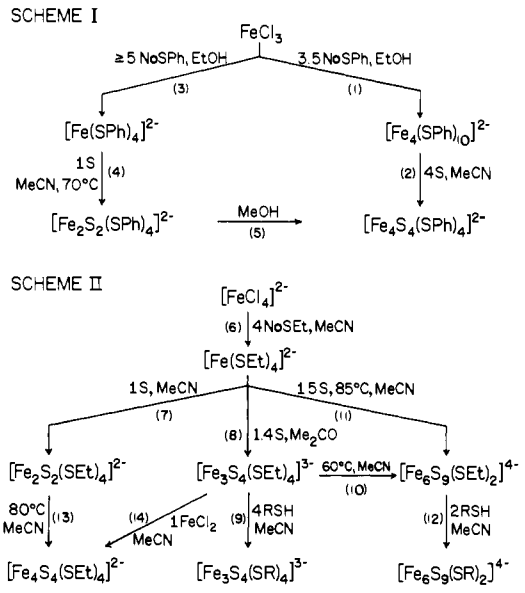

Figure 1. Reactions and products in systems based on $FeCl_3$/NaSPh and leading to the formation of Fe_2S_2 and Fe_4S_4 clusters (Scheme I[4]), and those in systems initially containing $[Fe(SEt)_4]^{2-}$ and affording Fe_2S_2, Fe_3S_4, and Fe_6S_9 clusters (Scheme II). In reaction 9 R = Ph and 2R = *o*-xyl, and in reaction 12 R = Ph.

stituted variant was reported earlier.[17] Although not a thiolate-containing cluster, $[Fe_6S_8(PEt_3)_6]^{2+}$,[18] comprised of a $[Fe_6(\mu_3\text{-}S)_8]^{2+}$ core formed from a slightly distorted S_8 cube with Fe atoms in the face-centered positions, is a significant addition to the set of oligomeric Fe–S compounds.

In our most recent attempts to develop synthetic routes to new Fe–S–SR clusters, we have examined the reactions of $FeCl_2$ or $[FeCl_4]^{2-}$ with 1–4 equiv of thiolate.[19] The intention has been to utilize the resultant Fe(II)–thiolate complexes as reactants with elemental sulfur, as in the cluster-forming redox reactions 2 and 4 in Scheme I. One of these complexes, $[Fe(SEt)_4]^{2-}$, has proven to be very reactive and has afforded direct entry to bi-, tri-, and hexanuclear clusters by means of the reactions outlined in Scheme II of Figure 1. Descriptions of these reactions and of the structures and other properties of the cluster products, with emphasis on tri- and hexanuclear species, are provided in this report.

Experimental Section

Preparation of Compounds. All operations were carried out under a pure dinitrogen or argon atmosphere using an inert atmosphere box and Schlenk techniques; solvents were degassed before use.

$(Et_4N)_2[Fe(SEt)_4]$. $(Et_4N)_2[FeCl_4]$[20] (46 g, 100 mmol) was added to a stirred slurry of 33.6 g (400 mmol) of NaSEt in 300 mL of acetonitrile. After the mixture was stirred for 30 min, during which time a yellow-brown solution and some white solid formed, the mixture was filtered. The solid collected by filtration (mainly NaCl) was washed until white with ~50 mL of acetonitrile. Removal of volatiles in vacuo afforded a thick brown oil, which was dissolved in ~100 mL of THF. When this solution was cooled to −20 °C, large off-white crystals separated and were collected by filtration. Addition of ether to the filtrate gave a further crop of the product, resulting in a typical combined crude yield of ~70%. This material was employed in subsequent reactions without further purification. Recyrstallization from acetonitrile/ether with cooling to −25 °C gave a product of analytical purity. Anal. Calcd for $C_{24}H_{60}FeN_2S_4$: C, 51.40; H, 10.78; Fe, 9.89; N, 4.99; S, 22.88. Found: C, 51.37; H, 10.54; Fe, 9.85; N, 5.13; S, 22.92. The Me_4N^+ and $Me_3NCH_2Ph^+$ salts were prepared by an analogous procedure. Salts of $[Fe(SEt)_4]^{2-}$ are extremely sensitive to oxygen, especially in solution; their preparation, manipulation, and reactions were conducted in an atmosphere containing <2 ppm O_2.

$(Me_3NCH_2Ph)_2[Fe_2S_2(SEt)_4]$. To a solution of 6.0 g (~10 mmol) of crude $(Me_3NCH_2Ph)_2[Fe(SEt)_4]$ (obtained as a powder by a procedure analogous to that of the preceding preparation) in 75 mL of acetonitrile was added 0.32 g (10 mmol) of sulfur. A dark brown solution formed, and black flakes separated within several minutes. The reaction mixture was stirred for 2 h and cooled to −25 °C. The product was collected by filtration, washed with acetonitrile and ether, and dried in vacuo; 2.9 g (80%) of flaky black microcrystals was obtained. Anal. Calcd for $C_{28}H_{52}Fe_2N_2S_6$: C, 46.66; H, 7.27; N, 3.89; S, 26.99. Found: C, 46.86; H, 7.00; N, 4.01; S, 26.07.

$(Et_4N)_3[Fe_3S_4(SEt)_4]$. A solution of 8.9 g (16 mmol) of $(Et_4N)_2[Fe(SEt)_4]$ in 100 mL of acetone was stirred with 0.71 g (22 mmol) of sulfur for 12 h. After the reaction mixture stood at room temperature for 24 h, black crystalline needles separated. These were collected, washed well with acetone until the washings were colorless, and dried in vacuo; 3.3 g (66%) of product was obtained. Anal. Calcd for $C_{32}H_{80}Fe_3N_3S_8$: C, 41.28; H, 8.66; Fe, 18.00; N, 4.51; S, 27.55. Found: C, 40.94; H, 8.40; Fe, 18.65; N, 4.90; S, 27.06. Crystal data: orthorhombic, a = 10.702 (4) Å, b = 27.099 (7) Å, c = 34.689 (9) Å.

$(Et_4N)_3[Fe_3S_4(SPh)_4]$. (a) By Ligand Substitution. Benzenethiol (0.470 g, 4.30 mmol) was added to a solution of 0.970 g (1.04 mmol) of $(Et_4N)_3[Fe_3S_4(SEt)_4]$ in 20 mL of acetonitrile. The reaction mixture was stirred for 10 min, and the flask was evacuated for several minutes to remove liberated ethanethiol. Diffusion of ~20 mL of ether into the solution followed by cooling caused separation of black crystals. These were collected by filtration, washed with ether, and dried in vacuo, affording 0.870 g (74%) of product. Anal. Calcd for $C_{48}H_{80}Fe_3N_3S_8$: C, 51.33; H, 7.18; Fe, 14.92; N, 3.74; S, 22.84. Found: C, 51.31; H, 6.61; Fe, 14.56; N, 3.74; S, 23.37.

(b) From $[Fe(SPh)_4]^{2-}$. Combination of 0.568 g (17.7 mmol) of sulfur and 8.90 g (11.8 mmol) of $(Et_4N)_2[Fe(SPh)_4]$[4] in 150 mL of acetonitrile resulted in a solution color change from pale yellow-green to purple-red and crystallization of $(Et_4N)_2[Fe_2S_2(SPh)_4]$.[21] The mixture was maintained at 80 °C for 22 h, allowed to cool slowly to room temperature, and then was cooled to −25 °C. Black platelike crystals of $(Et_4N)_2[Fe_2S_2(SPh)_4]$ were collected, washed with THF and ether, and dried in vacuo. Cooling of the combined washings and filtrate to −25 °C yielded fine black needles of $(Et_4N)_3[Fe_3S_4(SPh)_4]$. These were washed with ether and dried in vacuo to give 1.0 g (24%) of product, identical with that obtained by the preceding method.

$(Et_4N)_4[Fe_6S_9(SEt)_2]$. (a) From $[Fe(SEt)_4]^{2-}$. A solution of $(Et_4N)_2[Fe(SEt)_4]$ in 150 mL of acetonitrile was prepared in situ from 4.6 g (10 mmol) of $(Et_4N)_2[FeCl_4]$ and 3.2 g (40 mmol) of NaSEt. After removal of NaCl by filtration the filtrate was stirred with 0.48 g (15 mmol) of sulfur for 20 min. A cold finger (water-cooled) was inserted into the flask, and the solution was maintained at 85 °C for 24 h. It was cooled to room temperature, resulting in the separation of black crystalline flakes, and then kept at −20 °C for 24 h. The solid was collected by filtration, washed with 3:7 v/v acetonitrile/ether and then ether, and dried in vacuo. Black crystalline plates (1.35 g, 71%) were obtained. Anal. Calcd for $C_{36}H_{90}Fe_6N_4S_{11}$: C, 34.10; H, 7.16; Fe, 26.46; N, 4.42; S, 27.78. Found: C, 33.77; H, 6.65; Fe, 25.62; N, 4.39; S, 27.95.

(b) From $[Fe_3S_4(SEt)_4]^{3-}$. A solution of 0.930 g (1.00 mmol) of $(Et_4N)_3[Fe_3S_4(SEt)_4]_2$ in 125 mL of acetonitrile was heated at 60 °C for 36 h. The volume was reduced in vacuo to ~30 mL and cooled to −25 °C, resulting in the separation of black crystalline flakes. These were collected, washed with ether, and dried in vacuo to afford 0.200 g (32% based on Fe) of product identical with that obtained by the preceding method.

(n-$Bu_4N)_2[Fe_4S_4(SEt)_4]$ from $(Et_4N)_3[Fe_3S_4(SEt)_4]$. Anhydrous $FeCl_2$ (0.126 g, 0.99 mmol) was added to a stirred solution of 0.931 g (1.00 mmol) of $(Et_4N)_3[Fe_3S_4(SEt)_4]$ in 40 mL of acetonitrile. An immediate color change from red-brown to green-brown occurred. After the reaction mixture was stirred for 30 min 0.10 g (1.2 mmol) of NaSEt was added, and the mixture was stirred for a further 30 min. Then 0.65 g (2.0 mmol) of n-Bu_4NBr was added. A black crystalline material separated immediately. The mixture was stirred for 2 h and cooled to −20 °C for 24 h. The solid product was collected by filtration, washed thoroughly with 2:3 v/v acetonitrile/ether and then ether, and dried in vacuo. This procedure afforded 1.06 g of crude product, which was recrystallized from hot acetonitrile. After the washing and drying steps were repeated, 0.63 g (63%) of black crystals were obtained. This material was found to have spectroscopic properties identical with those of authentic $[Fe_4S_4(SEt)_4]^{2-}$ salts.[22,23]

(16) Hagen, K. S.; Christou, G.; Holm, R. H. *Inorg. Chem.* **1983**, *22*, 309. S_2-*o*-xyl = *o*-xylene-α,α'-dithiolate.
(17) Henkel, G.; Tremel, W.; Krebs, B. *Angew. Chem., Int. Ed. Engl.* **1981**, *20*, 1033.
(18) Cecconi, F.; Ghilardi, C. A.; Midollini, S. *J. Chem. Soc., Chem. Commun.* **1981**, 640.
(19) Hagen, K. S.; Holm, R. H. *J. Am. Chem. Soc.* **1982**, *104*, 5496.
(20) Gill, N. S.; Taylor, F. B. *Inorg. Synth.* **1967**, *9*, 136.
(21) Mayerle, J. J.; Denmark, S. E.; DePamphilis, B. V.; Ibers, J. A.; Holm, R. H. *J. Am. Chem. Soc.* **1975**, *97*, 1032.

Table I. Summary of Crystal Data, Intensity Collections, and Structure Refinements

quantity	$(Et_4N)_3[Fe_3S_4(SPh)_4]$	$(Et_4N)_4$-$[Fe_6S_9(SEt)_2]\cdot 4MeCN$
formula (mol wt)	$C_{48}H_{80}Fe_3N_3S_8$ (1123.25)	$C_{44}H_{102}Fe_6N_8S_{11}$ (1435.56)
a, Å	36.748 (4)	11.537 (3)
b, Å	9.114 (2)	11.706 (3)
c, Å	17.427 (4)	28.45 (1)
α, deg	90	98.14 (3)
β, deg	90	81.80 (3)
γ, deg	90	110.91 (2)
V, Å^3	5836 (7)	3536 (2)
cryst system	orthorhombic	triclinic
Z	4	2
d_{calcd}, g/cm^3	1.28	1.35
d_{obsd}, g/cm^3	1.28 (1)[a]	[b]
space group	$Pna2_1$	$P\bar{1}$
cryst dimens, mm	0.5 × 0.5 × 0.3	0.5 × 0.4 × 0.1
radiation	Mo K$\bar{\alpha}$ (λ 0.710 69 Å)	Mo K$\bar{\alpha}$ (λ 0.710 69 Å)
abs coeff, μ, cm^{-1}	10.4	15.4
scan speed,	2.9–29.3 ($\theta/2\theta$ scan)	2.0–29.3 ($\theta/2\theta$ scan)
scan range, deg	$1.5 + (2\theta K\alpha_2 - 2\theta K\alpha_1)$	$2.0 + (2\theta K\alpha_2 - 2\theta K\alpha_1)$
bckgrd/scan time ratio	0.25	0.25
data collected	$3° \leq 2\theta \leq 50°$ $(+h,+k,\pm l)$	$3° \leq 2\theta \leq 40°$ $(+h,\pm k,\pm l)$
unique data ($I > 3\sigma(I)$)	7657	4202
no. of variables	670	630
goodness of fit	1.14	1.26
R, %	3.9	4.1
R_w, %	4.1	4.4

[a] Measured in CCl_4/hexane. [b] Not accurately determinable because of solvate form.

Collection and Reduction of X-ray Data. Air-sensitive crystals of $(Et_4N)_3[Fe_3S_4(SPh)_4]$ and $(Et_4N)_4[Fe_6S_9(SEt)_2]\cdot 4MeCN$ were sealed in glass capillaries under argon and were mounted on a Nicolet R3m four-circle diffractometer for data collection and processing at ambient temperature using graphite-monochromatized Mo K$\bar{\alpha}$ radiation. Machine and crystal parameters are given in Table I. Three check reflection intensities were measured every 123 reflections and exhibited no decay with either crystal. The data were processed with the program XTAPE of the SHELXTL program package (Nicolet XRD Corp., Fremont, CA); an empirical absorption correction was applied to each data set.

(a) $(Et_4N)_3[Fe_3S_4(SPh)_4]$. Long black needles of this compound were obtained by diffusing ether into an acetonitrile solution. One crystal was cleaved to give a fragment of suitable dimensions. The orientation matrix and unit cell dimensions were calculated by least-squares treatment of 16 machine-centered reflections ($30° \leq 2\theta \leq 35°$). The systematic absences $0kl$ ($k + l \neq 2n$) and $h0l$ ($h \neq 2n$) indicated the space group to be either $Pna2_1$ or $Pnam$. Statistical analysis of intensities led to the former, noncentrosymmetric space group, and subsequent solution and refinement of the structure confirmed this choice.

(b) $(Et_4N)_4[Fe_6S_9(SEt)_2]\cdot 4MeCN$. Black crystals of this compound were grown by slow cooling of a reaction mixture in preparative method b. The orientation matrix and unit cell dimensions were calculated by least-squares treatment of 25 machine-centered reflections ($20° \leq 2\theta \leq 25°$). The centrosymmetric space group $P\bar{1}$ was chosen after inspection of a statistical analysis of intensities and was confirmed by successful solution and refinement of the structure.

Structure Solution and Refinement. (a) $(Et_4N)_3[Fe_3S_4(SPh)_4]$. The direct methods program SOLV revealed the positions of the three iron atoms. All remaining non-hydrogen atoms were found by successive difference Fourier maps. Isotropic refinement with phenyl rings fixed as rigid bodies converged at $R = 7.9\%$. The three iron and eight sulfur atoms were refined anisotropically to $R = 6.9\%$. Inverting the coordinates of all atoms reduced the R factor to 6.4%. All further refinements were performed on these coordinates with the z coordinate of Fe(1) fixed. Difference maps revealed four peaks of intensity greater than 1 e$^-$/Å^3 in the vicinity of the nitrogen atom of one cation. These peaks were assigned to disordered methylene carbon atoms. Their occupancies refined such that the sum of each disordered pair was unity. The average of the refined occupancies was 0.23. Convergence occurred at $R = 4.9\%$ with all but the disordered atoms refined anisotropically. Inclusion of hydrogen atoms at idealized positions in the anion and the two well-behaved cations, with temperature factors 1.2 times those of the bonded carbon atoms, resulted in the R factors in Table I.

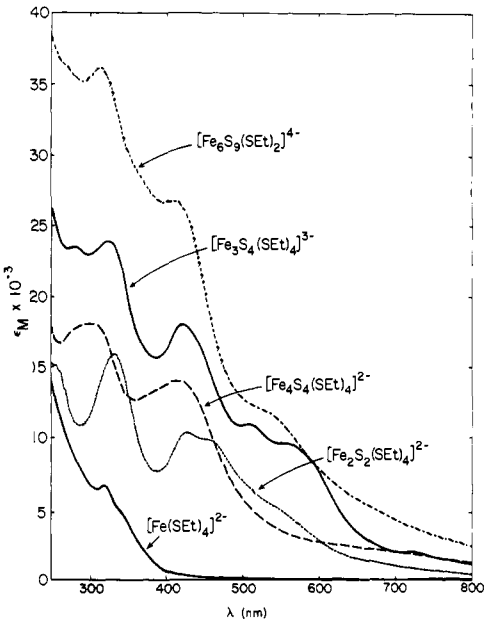

Figure 2. UV–visible absorption spectra of Fe–S–SEt complexes in acetonitrile solutions.

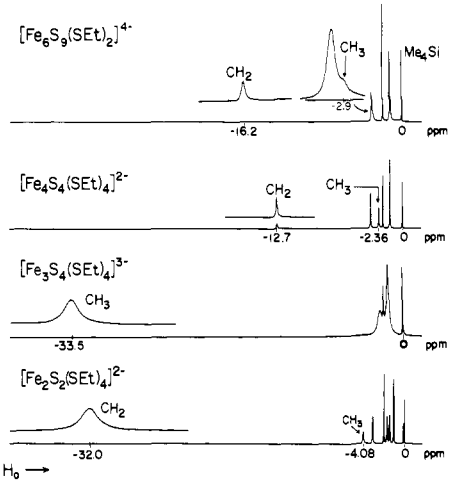

Figure 3. ^{1}H NMR spectra (300 MHz) of Fe–S–SEt complexes in CD_3CN solutions at ~27 °C. Peak assignments are indicated; cation and protio solvent signals are unlabeled. Inset resonances were recorded at higher gain.

(b) $(Et_4N)_4[Fe_6S_9(SEt)_2]\cdot 4MeCN$. The direct methods program SOLV revealed the positions of the six iron atoms. All remaining non-hydrogen atoms were found from successive difference maps on the partially refined structure. Isotropic refinement converged at $R = 8.3\%$ and an anisotropic treatment at $R = 5.1\%$. Hydrogen atoms were then included at their calculated positions with isotropic temperature factors set a 1.2 times those of the bonded carbon atoms. Two of the methylene carbon atoms of one cation were disordered and were refined as two pairs with fixed occupancies of 0.60 and 0.40. The final R factors are given in Table I.[24]

Other Physical Measurements. Determination of the physical properties of the compounds in Table II was performed under anaerobic conditions by using the procedures and instrumentation described elsewhere.[14,25] Magnetic susceptibilities of solid samples were measured by

(22) Holm, R. H.; Phillips, W. D.; Averill, B. A.; Mayerle, J. J.; Herskovitz, T. *J. Am. Chem. Soc.* **1974**, *96*, 2109.

(23) DePamphilis, B. V.; Averill, B. A.; Herskovitz, T.; Que, L., Jr.; Holm, R. H. *J. Am. Chem. Soc.* **1974**, *96*, 4159.

(24) See paragraph at the end of the article regarding supplementary structural material.

(25) Armstrong, W. H.; Mascharak, P. K.; Holm, R. H. *J. Am. Chem. Soc.* **1982**, *104*, 4373.

Table II. Properties of Fe-S-SR Complexes

compound	abs spectrum, λ, nm (ϵ_M)[a,b]	^{1}H shifts, ppm (~27 °C)[a,c]	μ_{Fe}, μ_B[d]	E, V[a] (vs. SCE)
$(Et_4N)_2[Fe(SEt)_4]$	316 (7150), 340 (sh), 2080 (100)[e]	−196 (CH_2), −10.0 (CH_3)	5.06	−1.08 (1−/2−)[g]
$(Me_3NCH_2Ph)_2[Fe_2S_2(SEt)_4]$	332 (15 600), 427 (10 100), 450 (9700)	−32.0 (CH_2), −4.08 (CH_3)	1.35	−1.31 (2−/3−)[g]
$(Et_4N)_3[Fe_3S_4(SEt)_4]$	282 (23 500), 325 (23 900), 422 (18 000), 508 (11 000), 560 (9500), 720 (1900)	−33.5 (CH_3)	3.39	−1.66 (3−/4−),[g] −1.79[f]
$(Et_4N)_3[Fe_3S_4(SPh)_4]$	268 (42 700), 323 (sh), 446 (17 500), 511 (14 800), 564 (12 400)	+27 (br, *o*-H), −37.8 (*m*-H), +38.8 (*p*-H)	3.12	−1.35 (3−/4−),[g] −1.48, −1.65[f]
$(Et_4N)_4[Fe_6S_9(SEt)_2]$	313 (35 700), 410 (26 400), 520 (sh, 12 000)	−16.2 (CH_2), ~−2.9 (CH_3)	1.07	−0.63 (3−/4−),[g] −1.75 (4−/5−)[g]

[a] Acetonitrile solutions. [b] M^{-1} cm^{-1}. [c] Signals downfield of Me_4Si reference are designated as negative. [d] ~296 K, solid state. [e] $^5E \rightarrow {}^5T_2$. [f] E_p (differential pulse polarography), reactions irreversible by cyclic voltammetry. [g] $E_{1/2} = {}^1/_2 (E_{p,c} + E_{p,a})$.

the Faraday method and are corrected for diamagnetism. Further experimental details are given in Table II.

Results and Discussion

In the following considerations of the reactions and products in Scheme II (Figure 1) containing reactions 6–14, initial reference is made to the spectroscopic, magnetic, and voltammetric properties compiled in Table II and to the distinctive absorption and ^{1}H NMR spectra of the various Fe–S–SEt complexes in Figures 2 and 3, respectively. With the exception of $[Fe_3S(SR)_6]^{2-}$[16,17] these figures display spectral information for all characterized structural types of Fe–S–SR clusters. These properties, especially the isotropically shifted ^{1}H NMR spectra, are diagnostic of structure at parity of thiolate ligand and provide a simple means of reaction product identification and assessment of purity. The reactions in Scheme II represent overall transformations to specified products, which were usually obtained in yields of ≳60% by strict adherence to the procedures given in the Experimental Section. As will be seen, these reactions as written do not imply the absence of other products.

$[Fe(SEt)_4]^{2-}$. Reaction 6 affords this species, the first example of a tetrakis(alkylmonothiolato)iron(II) monomer, in ~70% yield as its Et_4N^+ salt. Magnetic and spectral properties, including the $^5E \rightarrow {}^5T_2$ ligand-field transition at 2080 nm, are indicative of a tetrahedral structure. On the basis of its composition and structure $[Fe(SEt)_4]^{2-}$ is a synthetic analogue of the $Fe(S\text{-}Cys)_4$ unit of reduced rubredoxins. Because of the demonstrated suitability of $[Fe(S_2\text{-}o\text{-}xyl)_2]^{2-}$[26] and $[Fe(SPh)_4]^{2-}$[6] in this regard, this aspect was not pursued.[27] Attention was directed toward reactions with elemental sulfur in view of the highly reducing nature of $[Fe(SEt)_4]^{2-}$ ($E_{1/2}$(1−/2−) = −1.08 V) compared to $[Fe(SPh)_4]^{2-}$ (−0.53 V).

The reactivity properties of $[Fe(SEt)_4]^{2-}$ were initially examined in a reaction system containing its Et_4N^+ salt and 1.5 equiv of sulfur in acetonitrile. NMR spectra at various stages of reaction are presented in Figure 4. Within 20 min the resonances of $[Fe(SEt)_4]^{2-}$ diminished in intensity, and new features appeared at −4.08, −32.0, and −33.5 (sh) ppm. Heating at 60 °C for 1–12 h resulted in abolishment of the $[Fe(SEt)_4]^{2-}$ signals, an increase in the relative intensity of the −33.5 ppm component of the downfield feature, and the appearance of a resonance at −8.3 ppm. Maintenance of the system at 80 °C for up to 10.5 h caused progressive diminution of the downfield pair of signals and the −8.3 ppm resonance and the appearance and growth of new signals at −12.7 and −16.2 ppm. This behavior indicated the formation of at least four paramagnetic complexes. That having the −12.7 ppm signal was identified as $[Fe_4S_4(SEt)_4]^{2-}$ by comparison with an authentic sample.[22] The others could not be definitely identified at this stage; however, the −16.2 ppm feature is similar in position to that of the reaction product of authentic $[Fe_6S_9(S\text{-}t\text{-}Bu)_2]^{4-}$ with ethanethiol in Me_2SO.[14] These observations led to the development of syntheses of three new clusters and, thereafter, to the NMR spectral identifications in Figures 3 and 4.

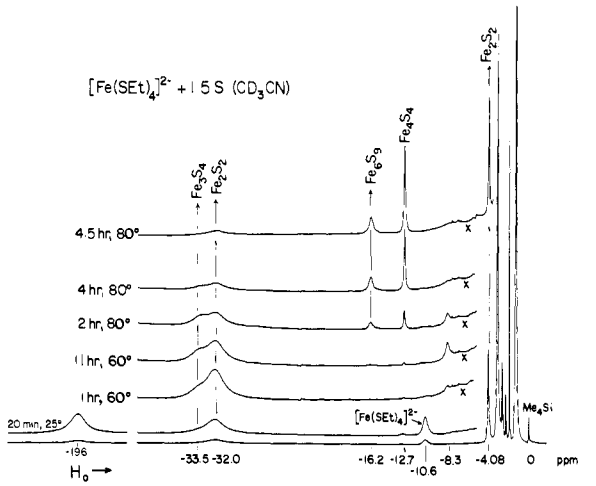

Figure 4. ^{1}H NMR spectra (300 MHz) of a reaction system initially containing ~0.10 M $(Et_4N)_2[Fe(SEt)_4]$ and 1.5 equiv of sulfur in CD_3CN. Spectra were recorded at 25 °C after maintaining the system at the indicated temperatures for the time intervals given. Signals due to the different cluster species are indicated. The relative intensities of the Fe_6S_9 signals are low because of the crystallization of the Et_4N^+ salt of this cluster. The −196 ppm signal of $[Fe(SEt)_4]^{2-}$ was recorded at higher gain than the remainder of the inset spectrum; X denotes a probe artifact.

$[Fe_2S_2(SEt)_4]^{2-}$. Reaction 7, between $(Me_3NCH_2Ph)_2[Fe(SEt)_4]$ and 1 equiv of sulfur, proceeds smoothly at ambient temperature and affords an 80% yield of $(Me_3NCH_2Ph)_2[Fe_2S_2(SEt)_4]$.[28] Owing to its low solubility this compound largely precipitates as the anion is generated. $[Fe_2S_2(SEt)_4]^{2-}$ is the initial species formed in the $[Fe(SEt)_4]^{2-}$/S reaction and gives rise to the −32.0 (CH_2) and −4.08 (CH_3) signals in Figure 4. It was identified by elemental analysis and correspondence with the properties of $[Fe_2S_2(S_2\text{-}o\text{-}xyl)_2]^{2-}$, which has been studied in detail.[21,29,30] Along with the latter species, $[Fe_2S_2(SEt)_4]^{2-}$ is a synthetic analogue of the $Fe_2S_2(S\text{-}Cys)_4$ units in oxidized ferredoxins. The absorption spectrum of $[Fe_2S_2(SEt)_4]^{2-}$ is virtually identical with that of the oxidized protein chromophore.[31] Reaction 7 is foreshadowed by the analogous formation of $[Fe_2S_2(SPh)_4]^{2-}$ in reaction 4 of Scheme I.

$[Fe_3S_4(SR)_4]^{3-}$. (a) Synthesis. Reaction 8, conducted in acetone between $(Et_4N)_2[Fe(SEt)_4]$ and ~1.4 equiv of sulfur, gave a black crystalline solid corresponding to the composition $(Et_4N)_3[Fe_3S_4(SEt)_4]$ (66% yield). The other reaction product was identified as $[Fe_2S_2(SEt)_4]^{2-}$, whose Et_4N^+ salt is sufficiently

(26) Lane, R. W.; Ibers, J. A.; Frankel, R. B.; Papaefthymiou, G. C.; Holm, R. H. *J. Am. Chem. Soc.* **1977**, *99*, 84.

(27) However, the −196 ppm shift of the broad CH_2 resonance accounts for the lack of detection of S–CH_2 signals of reduced rubredoxin. Signals in this region lie far outside the sweep range of the protein experiments: Phillips, W. D.; Poe, M.; Weiher, J. F.; McDonald, C. C.; Lovenberg, W. *Nature (London)* **1970**, *227*, 574.

(28) Salts of more common quaternary cations such as Et_4N^+ are highly soluble in acetonitrile and difficult to isolate.

(29) Gillum, W. O.; Frankel, R. B.; Foner, S.; Holm, R. H. *Inorg. Chem.* **1976**, *15*, 1095.

(30) Mascharak, P. K.; Papaefthymiou, G. C.; Frankel, R. B.; Holm, R. H. *J. Am. Chem. Soc.* **1981**, *103*, 6110.

(31) Palmer, G.; Brintzinger, H.; Estabrook, R. W. *Biochemistry* **1967**, *6*, 1658. Mayhew, S. G.; Petering, D.; Palmer, G.; Foust, G. P. *J. Biol. Chem.* **1969**, *244*, 2830.

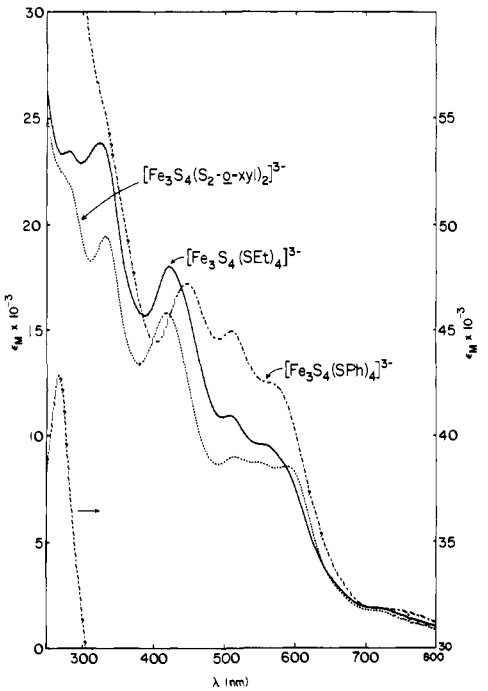

Figure 5. Absorption spectra of $[Fe_3S_4(SR)_4]^{3-}$ clusters in acetonitrile solution. The arrow refers to the right-hand ϵ_M axis. The species formulated as $[Fe_3S_4(S_2\text{-}o\text{-xyl})_2]^{3-}$ was generated by ligand exchange (see text); its extinction coefficient scale is of only semiquantitative significance.

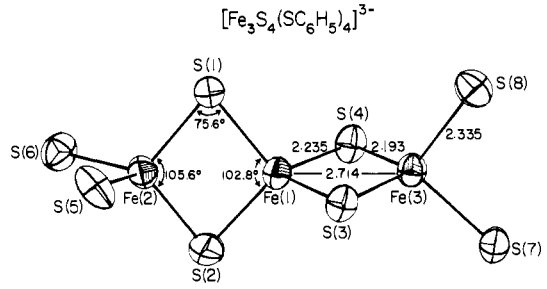

Figure 6. Structure of the Fe_3S_8 portion of $[Fe_3S_4(SPh)_4]^{3-}$ as its Et_4N^+ salt, showing the atom labeling scheme, 50% probability ellipsoids, and certain interatomic distances and angles averaged under idealized D_{2d} symmetry.

soluble to allow the former product to be isolated in analytical purity. In reaction 9 $[Fe_3S_4(SEt)_4]^{3-}$ underwent thiolate ligand substitution with benzenethiol to give $(Et_4N)_3[Fe_3S_4(SPh)_4]$ in 74% yield. The −33.5 ppm resonance in Figure 4 is due to $[Fe_3S_4(SEt)_4]^{3-}$. A species of probable formulation $[Fe_3S_4(S_2\text{-}o\text{-xyl})_2]^{3-}$, on the basis of spectral absorption similarities with $[Fe_3S_4(SEt)_4]^{3-}$ shown in Figure 5, was generated in solution by reaction 9 using 2 mol equiv of o-xyl$(SH)_2$.[21] The former showed no resonance in the vicinity of −30 ppm, indicating that the observed downfield feature of $[Fe_3S_4(SEt)_4]^{3-}$ arises from methyl groups. Presumably the methylene resonances of both clusters are severely broadened by paramagnetic relaxation effects and thus far have not been detected.

$(Et_4N)_3[Fe_3S_4(SPh)_4]$ was alternatively obtained by the reaction of $[Fe(SPh)_4]^{2-}$ and 1.5 equiv of sulfur in acetonitrile. The yield (24%) is low but the one-step procedure is convenient. Absorption spectra of the three $[Fe_3S_4(SR)_4]^{3-}$ clusters, presented in Figure 5, suggest the presence of similar chromophores whose structural nature could not be deduced from this or other properties (Table II). Consequently, an X-ray structural analysis of one member of the set was performed.

(b) Structure of $(Et_4N)_3[Fe_3S_4(SPh)_4]$. The crystal structure of this compound consists of well-separated cations and anions. Positional parameters and selected interatomic distances and angles are listed in Tables III and IV, respectively. Cation and phenyl group structural features are unexceptional.[24] The structure of the Fe_3S_8 portion of the anion, briefly described earlier,[19] is

Table III. Positional Parameters for $[Fe_3S_4(SPh)_4]^{3-}$

atom	x	y	z
Fe(1)	0.85163 (2)[a]	0.29976 (7)	0.13688 (4)
Fe(2)	0.90974 (2)	0.30594 (8)	0.04190 (4)
Fe(3)	0.79173 (2)	0.25856 (7)	0.22656 (4)
S(1)	0.85302 (3)	0.26790 (14)	0.01027 (7)
S(2)	0.90898 (4)	0.36555 (17)	0.16419 (8)
S(3)	0.83404 (4)	0.09665 (13)	0.19933 (7)
S(4)	0.80936 (4)	0.46233 (13)	0.17108 (8)
S(5)	0.93566 (4)	0.07982 (16)	0.00941 (11)
S(6)	0.93880 (4)	0.49372 (16)	−0.02409 (8)
S(7)	0.78209 (4)	0.29348 (15)	0.35873 (8)
S(8)	0.73654 (4)	0.15988 (15)	0.18632 (9)
C(1)S(5)	0.9826 (2)	0.0701 (8)	0.0230 (3)
C(2)S(5)	0.9994 (2)	−0.0631 (9)	0.0055 (4)
C(3)S(5)	1.0374 (3)	−0.0728 (15)	0.0147 (5)
C(4)S(5)	1.0574 (2)	0.0469 (16)	0.0395 (5)
C(5)S(5)	1.0411 (2)	0.1724 (16)	0.0567 (5)
C(6)S(5)	1.0030 (2)	0.1871 (10)	0.0481 (5)
C(1)S(6)	0.9293 (2)	0.4802 (6)	−0.1228 (3)
C(2)S(6)	0.9093 (2)	0.3681 (8)	−0.1570 (4)
C(3)S(6)	0.9035 (2)	0.3669 (10)	−0.2350 (4)
C(4)S(6)	0.9163 (2)	0.4786 (10)	−0.2792 (5)
C(5)S(6)	0.9354 (3)	0.5925 (10)	−0.2472 (4)
C(6)S(6)	0.9415 (2)	0.5921 (7)	−0.1712 (4)
C(1)S(7)	0.8230 (1)	0.3262 (5)	0.4083 (3)
C(2)S(7)	0.8574 (2)	0.3234 (6)	0.3730 (3)
C(3)S(7)	0.8886 (2)	0.3554 (8)	0.4156 (4)
C(4)S(7)	0.8866 (2)	0.3839 (9)	0.4912 (4)
C(5)S(7)	0.8539 (2)	0.3867 (9)	0.5263 (4)
C(6)S(7)	0.8226 (2)	0.3565 (7)	0.4865 (3)
C(1)S(8)	0.7023 (1)	0.2934 (6)	0.1775 (3)
C(2)S(8)	0.6659 (2)	0.2483 (7)	0.1757 (3)
C(3)S(8)	0.6376 (2)	0.3504 (8)	0.1677 (4)
C(4)S(8)	0.6449 (2)	0.4946 (8)	0.1596 (3)
C(5)S(8)	0.6802 (2)	0.5423 (8)	0.1598 (4)
C(6)S(8)	0.7090 (2)	0.4430 (7)	0.1679 (3)

[a] Estimated standard deviations in parentheses in this and succeeding tables. [b] Phenyl ring numbering scheme:

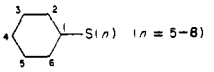

Table IV. Selected Interatomic Distances (Å) and Angles (deg) in $[Fe_3S_4(SPh)_4]^{3-}$

Fe(1)···Fe(2)	2.703 (2)	Fe(2)-Fe(1)-Fe(3)	172.9 (1)
Fe(1)···Fe(3)	2.725 (2)	S(1)-Fe(1)-S(2)	102.9 (1)
mean	2.714	S(3)-Fe(1)-S(4)	102.6 (1)
Fe(1)-S(1)	2.226 (2)	S(1)-Fe(1)-S(3)	112.3 (1)
Fe(1)-S(2)	2.243 (2)	S(1)-Fe(1)-S(4)	111.6 (1)
Fe(1)-S(3)	2.242 (2)	S(2)-Fe(1)-S(3)	112.9 (1)
Fe(1)-S(4)	2.227 (2)	S(2)-Fe(1)-S(4)	114.9 (1)
mean	2.235 (9)[a]	S(1)-Fe(2)-S(2)	105.8 (1)
Fe(2)-S(1)	2.184 (2)	S(3)-Fe(3)-S(4)	105.4 (1)
Fe(2)-S(2)	2.201 (2)	Fe(1)-S(1)-Fe(2)	75.6 (1)
Fe(3)-S(3)	2.194 (2)	Fe(1)-S(2)-Fe(2)	74.9 (1)
Fe(3)-S(4)	2.192 (2)	Fe(1)-S(3)-Fe(3)	75.8 (1)
mean	2.193 (7)	Fe(1)-S(4)-Fe(3)	76.1 (1)
Fe(2)-S(5)	2.339 (2)	S(5)-Fe(2)-S(6)	110.0 (1)
Fe(2)-S(6)	2.322 (2)	S(7)-Fe(3)-S(8)	102.5 (1)
Fe(3)-S(7)	2.353 (2)	S(1)-Fe(2)-S(5)	100.8 (1)
Fe(3)-S(8)	2.326 (2)	S(1)-Fe(2)-S(6)	115.5 (1)
mean	2.335 (14)	S(2)-Fe(2)-S(5)	117.2 (1)
C(1)S(5)-S(5)	1.746 (5)	S(2)-Fe(2)-S(6)	107.7 (1)
C(1)S(6)-S(6)	1.764 (6)	S(3)-Fe(3)-S(7)	114.2 (1)
C(1)S(7)-S(7)	1.758 (5)	S(3)-Fe(3)-S(8)	107.0 (1)
C(1)S(8)-S(8)	1.762 (5)	S(4)-Fe(3)-S(7)	111.2 (1)
mean	1.758 (8)	S(4)-Fe(3)-S(8)	116.9 (1)
C-C, range	1.33 (2)-1.42 (1)		
mean of 24	1.38 (2)		

[a] The standard deviation of the mean was estimated from $\sigma \approx s = [(\Sigma x_i^2 - n\bar{x}^2)/(n-1)]^{1/2}$.

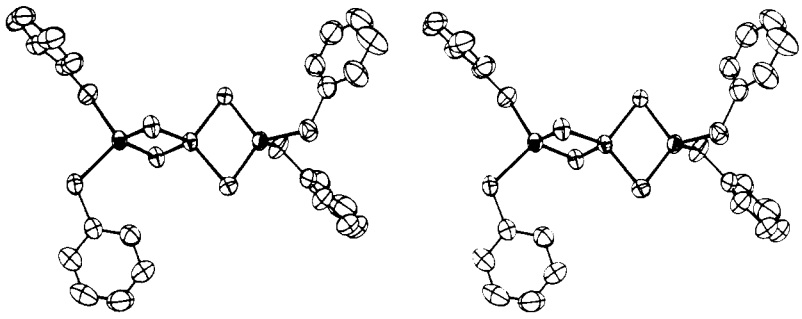

Figure 7. Stereoview of $[Fe_3S_4(SPh)_4]^{3-}$ with 50% probability ellipsoids.

presented in Figure 6; a stereoview of the entire anion is provided in Figure 7. No symmetry is imposed on the anion, but the Fe_3S_8 portion approaches idealized D_{2d} symmetry, under which the metric data in Table IV are organized. The structure consists of a $[Fe_3S_4]^+$ core unit, with Fe(2,3) terminally coordinated by two thiolate ligands. Each Fe atom occupies an approximately tetrahedral site. The Fe atoms approach collinearity (∠Fe(2)–Fe(1)–Fe(3) = 172.9 (1)°). The two Fe_2S_2 core subunits are not exactly planar; displacements from unweighted least-squares planes are ±0.024 Å for Fe(1)–S(3)–Fe(3)–S(4) and ±0.064 Å for Fe(1)–S(1)–Fe(2)–S(2). These planes are disposed at a dihedral angle of 89.4°. Mean values of bond angles and distances (including terminal Fe–S bond lengths) are within 1° and 0.04 Å of the corresponding parameters of $[Fe_2S_2(S_2\text{-}o\text{-xyl})_2]^{2-}$ and $[Fe_2S_2(S\text{-}p\text{-}C_6H_4Me)_4]^{2-}$.[1,21] The Fe···Fe separations of 2.698 (1) and 2.691 (1) Å, respectively, in these two species are only slightly shorter than the values for $[Fe_3S_4(SPh)_4]^{3-}$ (2.703 (2), 2.725 (2) Å). Consequently, the $[Fe_3S_4]^+$ core can be described in terms of two $Fe^{III}S_2$ fragments of unexceptional dimensions joined by a central Fe(III) atom. There is no structural feature that suggests that the central $Fe(1)S_4$ portion should be regarded as an oxidized tetrathioferrate, e.g., as the (unknown) sulfido analogue of a species such as FeO_4^{2-}.[32] In such a case shorter Fe–S distances are expected, as have been observed in complexes of tetrathiometalates(V–VII).[33] In fact, Fe(1)–S distances are longer than Fe(2,3)–S core distances.

The $[Fe_3S_4]^+$ core is a new structural element in discrete Fe–S clusters. It may be considered as a small solubilized fraction of the chains of the edge-shared $Fe(\mu_2\text{-}S)_4$ tetrahedra present in the extended structures of $KFeS_2$[34,35] and $CsFeS_2$.[35] The former, a linear chain antiferromagnet,[36] was considered as an early model of the sites of 2-Fe ferredoxins. Similar chains of tetrahedra are found in $Ba_5Fe_9S_{18}$.[37] In $Ba_7Fe_6S_{14}$[38] the structure consists of a central FeS_4 tetrahedron which shares edges with two other tetrahedra, the $Fe_3S_6S_{2/2}$ clusters being linked by corner-sharing. The latter two materials contain Fe in a mean fractional oxidation state. While the $[Fe_3S_4]^+$ core enjoys precedents of a sort in these polymeric compounds, it is only one of three reasonable arrangements for this stoichiometry with tetrahedral Fe sites. The others are **1**, in effect a distorted Fe_4S_4 cubane-type unit minus one Fe atom, and the stirrup-shaped configuration **2**. Neither has been realized experimentally.[39]

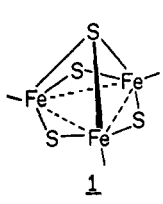

1

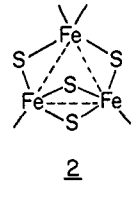

2

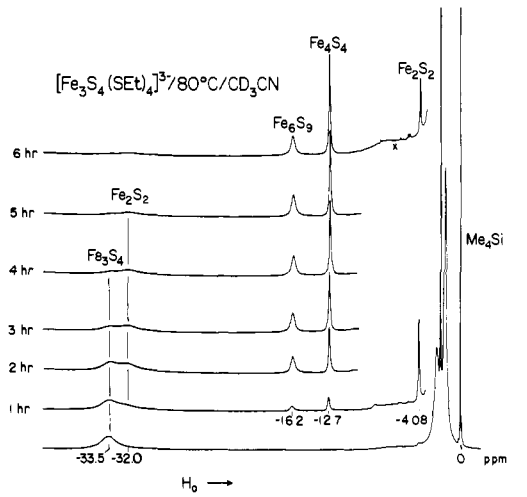

Figure 8. ^1H NMR spectra (300 MHz) of a CD_3CN solution initially containing ~50 mM $(Et_4N)_3[Fe_3S_4(SEt)_4]$ heated at 80 °C for 1-h intervals. After each interval the solution was cooled to ~25 °C for 10–15 min, and the spectrum was recorded. Intensities in the 6-h spectrum are not indicative of relative amounts of clusters because a significant quantity of $(Et_4N)_4[Fe_6S_9(SEt)_2]$ had crystallized from solution. Signal assignments are indicated; X denotes a probe artifact.

(c) Other Properties. The three Fe_3S_4 clusters each exhibit several reduction steps that in cyclic voltammetry appear to be irreversible. The first of these is presumably the initial reduction of the intact cluster (3–/4–) and is so designated in Table II. Both the irreversibility and the quite negative values of the first reduction potential do not presage successful isolation of reduced clusters that retain the linear $Fe_3(\mu_2\text{-}S)_4$ core arrangement. Freshly prepared solutions of $[Fe_3S_4(SEt)_4]^{3-}$ in acetonitrile afford EPR spectra with a symmetrical resonance centered at $g \cong 4.2$ at ~7 K, suggestive of a molecular $S = {}^5/_2$ ground state. No features are observed near $g = 2$. Magnetic moments per Fe atom, μ_{Fe}, for solid and solution samples are reduced below that (5.92 μ_B) for magnetically dilute Fe(III) and are consistent with the spin-only value (3.42 μ_B) for a molecular sextet state. Spin-coupled interactions are common to all Fe–S–SR clusters and for Fe_2S_2[29] and Fe_4S_4[40] clusters result in antiferromagnetism. Magnetic properties of $[Fe_4S_4(SR)_4]^{2-,3-}$ have been interpreted theoretically on this basis.[40] Further consideration of the electronic properties of $[Fe_3S_4(SR)_4]^{3-}$ species is deferred to a later report.

(32) Cotton, F. A.; Wilkinson, G. "Advanced Inorganic Chemistry", 4th ed.; Wiley: New York, 1980; pp 765–766.
(33) Müller, A.; Diemann, E.; Jostes, R.; Bögge, H. *Angew. Chem., Int. Ed. Engl.* **1981**, *20*, 934.
(34) Boon, J. W.; MacGillavry, C. H. *Recl. Trav. Chim. Pays*-Bas **1942**, *61*, 910.
(35) Bronger, W. *Z. Anorg. Allg. Chem.* **1968**, *359*, 225.
(36) Sweeney, W. V.; Coffman, R. E. *Biochim. Biophys. Acta* **1972**, *286*, 26.
(37) Grey, I. E. *Acta Crystallogr., Sect. B* **1975**, *B31*, 45.
(38) Grey, I. E.; Hong, H.; Steinfink, H. *Inorg. Chem.* **1971**, *10*, 340.
(39) Among Fe–S clusters the "inverse" arrangement of core atoms in **1** is found with $[Fe_4(NO)_7(\mu_3\text{-}S)_3]^-$: Chu, C. T.-W.; Dahl, L. F. *Inorg. Chem.* **1977**, *16*, 3245. Structure **2**, as a possible configuration of the 3-Fe sites in proteins, has been independently conceived: Beinert, H.; Emptage, M. H.; Dreyer, J.-L.; Scott, R. A.; Hahn, J. E.; Hodgson, K. O.; Thomson, A. J. *Proc. Natl. Acad. Sci. U.S.A.* **1980**, *80*, 393. **Note Added in Proof**: Results described in this reference show that the 3-Fe cluster in aconitase has the core composition Fe_3S_4 and one or more Fe···Fe separations of ~2.7 Å.
(40) Papaefthymiou, G. C.; Laskowski, E. J.; Frota-Pessôa, S.; Frankel, R. B.; Holm, R. H. *Inorg. Chem.* **1982**, *21*, 1723.

Table V. Positional Parameters for $[Fe_6S_9(SEt)_2]^{4-}$

atom	x	y	z
Fe(1)	0.6024 (1)	0.3695 (1)	0.8303 (1)
Fe(2)	0.5633 (1)	0.3740 (1)	0.7352 (1)
Fe(3)	0.7073 (1)	0.2327 (1)	0.7052 (1)
Fe(4)	0.7465 (1)	0.2292 (1)	0.8002 (1)
Fe(5)	0.7245 (1)	0.3139 (1)	0.8940 (1)
Fe(6)	0.6157 (1)	0.3173 (1)	0.6402 (1)
S(1)	0.7517 (2)	0.3989 (2)	0.7641 (1)
S(2)	0.5681 (2)	0.1766 (2)	0.8534 (1)
S(3)	0.4395 (2)	0.3870 (2)	0.8021 (1)
S(4)	0.5010 (2)	0.1816 (2)	0.6926 (1)
S(5)	0.7437 (2)	0.0885 (2)	0.7378 (1)
S(6)	0.6953 (3)	0.4926 (2)	0.8913 (1)
S(7)	0.6044 (2)	0.4966 (2)	0.6770 (1)
S(8)	0.8041 (2)	0.2973 (2)	0.6360 (1)
S(9)	0.8935 (2)	0.2907 (2)	0.8497 (1)
S(10)	0.7176 (3)	0.2810 (3)	0.9716 (1)
S(11)	0.5377 (3)	0.2711 (2)	0.5674 (1)
C(1)S(10)	0.7088 (19)	0.1290 (11)	0.9676 (5)
C(2)S(10)	0.7173 (15)	0.0755 (12)	1.0072 (5)
C(1)S(11)	0.5747 (12)	0.4252 (11)	0.5459 (4)
C(2)S(11)	0.6953 (12)	0.4789 (13)	0.5278 (5)

$[Fe_6S_9(SEt)_2]^{4-}$. (a) Synthesis. A crystalline solid of composition $(Et_4N)_4[Fe_6S_9(SEt)_2]$ was obtained by two methods, reactions 10 and 11. In reaction 10 a solution of $(Et_4N)_3[Fe_3S_4(SEt)_4]$ in acetonitrile was heated at 60–80 °C, and the product crystallized in 32% yield. As seen in the NMR spectra of Figure 8 there is initial formation of some $[Fe_2S_2(SEt)_4]^{2-}$ and, at longer times, elimination of the starting cluster and growth of $[Fe_4S_4(SEt)_4]^{2-}$ and the −16.2 ppm resonance. The latter was identified as the CH_2 resonance of $[Fe_6S_9(SEt)_2]^{4-}$; the CH_3 resonance occurs as a shoulder at −2.9 ppm on the cation signal (Figure 3). Reaction 11, between $(Et_4N)_2[Fe(SEt)_4]$ generated in situ and 1.5 equiv of sulfur at elevated temperature, resulted in a 71% yield. In both reactions isolation of product was greatly facilitated by its relatively low solubility compared to the Et_4N^+ salts of other clusters. The properties of the product (Table II) are similar to those of $[Fe_6S_9(S\text{-}t\text{-}Bu)_2]^{4-}$.[14] These extend to reversible one-electron oxidation and reduction processes and to the ligand-substitution reaction 12 with benzenethiol, which generates a cluster previously identified as $[Fe_6S_9(SPh)_2]^{4-}$. Because of different synthetic procedures and the few examples of Fe_6S_9 clusters, structural confirmation was sought by X-ray analysis.

(b) Structure of $(Et_4N)_4[Fe_6S_9(SEt)_2]\cdot 4MeCN$. Upon slow cooling of the mixture from reaction 10 and omission of the washing and drying steps, the product was isolated as an acetonitrile tetrasolvate. The crystal structure of the compound is composed of discrete cations, anions, and solvate molecules. Positional parameters and selected interatomic distances and angles of the anion are presented in Tables V and VI,[24] respectively. The anion structure, displayed in two perspectives in Figure 9, has the same topology as the Fe_6S_{11} portions of $[Fe_6S_9(SR)_2]^{4-}$ (R = *t*-Bu,[14] CH_2Ph[15]). A stereoview of one of these clusters is available elsewhere.[14] Because the structure of $[Fe_6S_9(S\text{-}t\text{-}Bu)_2]^{4-}$ has been described at length earlier,[13,14] only a brief summary of the principal structural features of $[Fe_6S_9(SEt)_2]^{4-}$ is given here. (i) No symmetry is imposed on the cluster, but it closely approaches idealized C_{2v} symmetry, with the C_2 axis containing S(1) and perpendicular to the Fe(1–4) unweighted least-squares plane (atom displacements of ±0.002 Å). (ii) The $[Fe_6S_9]^{2-}$ core consists of Fe_2S_2 fragments fused in the arrangement $4Fe_2(\mu_2\text{-}S)(\mu_3\text{-}S) + 2Fe_2(\mu_2\text{-}S)(\mu_4\text{-}S) + 2Fe_2(\mu_3\text{-}S)(\mu_4\text{-}S)$. (iii) Corresponding bond distances and angles in the Fe_6S_{11} portions of $[Fe_6S_9(SR)_2]^{4-}$ (R = Et, *t*-Bu) do not differ by more than 0.025 Å and 1.1° (and usually by less); hence the two clusters are essentially isometric. (iv) Although $[Fe_6S_9(SEt)_2]^{4-}$ is a mixed-valence species (4Fe(III) + 2Fe(II)), there is no clear structural evidence for localized Fe(II,III) sites. Henkel et al.[15] have described the topologically "closed parent compound" of Fe_6S_9 clusters as a species containing the $Fe_8(\mu_4\text{-}S)_6$ core of O_h symmetry with tetrahedral coordination at each Fe site completed by a thiolate ligand. This arrangement

Table VI. Selected Interatomic Distances (Å) and Angles (deg) in $[Fe_6S_9(SEt)_2]^{4-}$

Fe-μ_2S		Fe-μ_2S-Fe	
Fe(1)-S(6)	2.225 (3)	Fe(1)-S(6)-Fe(5)	74.9 (1)
Fe(2)-S(7)	2.231 (3)	Fe(2)-S(7)-Fe(6)	74.9 (1)
Fe(3)-S(8)	2.211 (2)	Fe(3)-S(8)-Fe(6)	74.7 (1)
Fe(4)-S(9)	2.212 (3)	Fe(4)-S(9)-Fe(5)	75.2 (1)
mean	2.220 (10)[a]	mean	74.9
Fe(1)-S(3)	2.230 (3)	Fe(1)-S(3)-Fe(2)	78.3 (1)
Fe(2)-S(3)	2.234 (2)	Fe(3)-S(5)-Fe(4)	78.1 (1)
Fe(3)-S(5)	2.224 (3)	mean	78.2
Fe(4)-S(5)	2.240 (2)		
mean	2.232 (7)	Fe-μ_3S-Fe	
Fe(5)-S(6)	2.248 (3)	Fe(1)-S(2)-Fe(5)	72.6 (1)
Fe(5)-S(9)	2.245 (3)	Fe(2)-S(4)-Fe(6)	73.0 (1)
Fe(6)-S(7)	2.248 (3)	Fe(3)-S(4)-Fe(6)	72.8 (1)
Fe(6)-S(8)	2.253 (3)	Fe(4)-S(2)-Fe(5)	72.6 (1)
mean	2.249 (3)	mean	72.8
		Fe(1)-S(2)-Fe(4)	71.4 (1)
Fe-μ_3S		Fe(2)-S(4)-Fe(3)	72.0 (1)
Fe(1)-S(2)	2.321 (3)	mean	71.7
Fe(2)-S(4)	2.319 (2)		
Fe(3)-S(4)	2.306 (2)	Fe-μ_4S-Fe	
Fe(4)-S(2)	2.318 (2)	Fe(1)-S(1)-Fe(2)	74.1 (1)
mean	2.316 (7)	Fe(3)-S(1)-Fe(4)	73.9 (1)
		mean	74.0
Fe(5)-S(2)	2.274 (2)	Fe(1)-S(1)-Fe(4)	70.7 (1)
Fe(6)-S(4)	2.259 (2)	Fe(2)-S(1)-Fe(3)	71.0 (1)
mean	2.267	mean	70.9
		Fe(1)-S(1)-Fe(3)	113.2 (1)
Fe-μ_4S		Fe(2)-S(1)-Fe(4)	113.5 (1)
Fe(1)-S(1)	2.339 (2)	mean	113.4
Fe(2)-S(1)	2.340 (3)		
Fe(3)-S(1)	2.338 (2)	S-Fe-μ_2S	
Fe(4)-S(1)	2.343 (3)	S(10)-Fe(5)-S(6)	109.3 (1)
mean	2.340 (2)	S(10)-Fe(5)-S(9)	112.1 (1)
		S(11)-Fe(6)-S(7)	112.1 (1)
Fe-SEt		S(11)-Fe(6)-S(8)	112.1 (1)
Fe(5)-S(10)	2.280 (3)	mean	111.4
Fe(6)-S(11)	2.293 (3)		
mean	2.287	S-Fe-μ_3S	
		S(10)-Fe(5)-S(2)	115.1 (1)
Fe···Fe		S(11)-Fe(6)-S(4)	112.1 (1)
Fe(1)-Fe(4)	2.708 (2)		
Fe(2)-Fe(3)	2.717 (2)	μ_2S-Fe-μ_2S	
mean	2.713	S(6)-Fe(5)-S(9)	115.9 (1)
		S(7)-Fe(6)-S(8)	115.0 (1)
Fe(1)-Fe(2)	2.819 (2)	S(3)-Fe(1)-S(6)	122.9 (1)
Fe(3)-Fe(4)	2.813 (2)	S(3)-Fe(2)-S(7)	124.0 (1)
mean	2.816	S(5)-Fe(3)-S(8)	122.1 (1)
		S(5)-Fe(4)-S(9)	122.5 (1)
Fe(1)-Fe(5)	2.720 (2)	mean	122.9
Fe(2)-Fe(6)	2.724 (2)		
Fe(3)-Fe(6)	2.709 (2)	μ_2S-Fe-μ_3S	
Fe(4)-Fe(5)	2.720 (2)	S(6)-Fe(1)-S(2)	101.7 (1)
mean	2.718 (6)	S(7)-Fe(2)-S(4)	101.3 (1)
		S(8)-Fe(3)-S(4)	101.8 (1)
C-S		S(9)-Fe(4)-S(2)	101.1 (1)
C(1)S(10)-S(10)	1.73 (2)	mean	101.5
C(1)S(11)-S(11)	1.87 (1)		
mean	1.80	S(3)-Fe(1)-S(2)	114.4 (1)
		S(3)-Fe(2)-S(4)	113.3 (1)
μ_2S-Fe-μ_4S		S(5)-Fe(3)-S(4)	113.1 (1)
S(3)-Fe(1)-S(1)	102.7 (1)	S(5)-Fe(4)-S(2)	114.0 (1)
S(3)-Fe(2)-S(1)	102.6 (1)	mean	113.7
S(5)-Fe(3)-S(1)	103.2 (1)		
S(5)-Fe(4)-S(1)	102.5 (1)	S(6)-Fe(5)-S(2)	102.6 (1)
mean	102.8	S(9)-Fe(5)-S(2)	101.4 (1)
		S(7)-Fe(6)-S(4)	102.6 (1)
S(6)-Fe(1)-S(1)	106.8 (1)	S(8)-Fe(6)-S(4)	101.9 (1)
S(7)-Fe(2)-S(1)	108.2 (1)	mean	102.1
S(8)-Fe(3)-S(1)	109.0 (1)		
S(9)-Fe(4)-S(1)	108.7 (1)	μ_3S-Fe-μ_4S	
mean	108.2	S(2)-Fe(1)-S(1)	107.5 (1)
		S(4)-Fe(2)-S(1)	106.5 (1)
		S(4)-Fe(3)-S(1)	107.0 (1)
		S(2)-Fe(4)-S(1)	107.5 (1)
		mean	107.1

[a] Standard deviation of the mean calculated as in Table IV; when no value is given with the mean of more than two quantities, the variations exceed those expected for a sample taken from the same population.

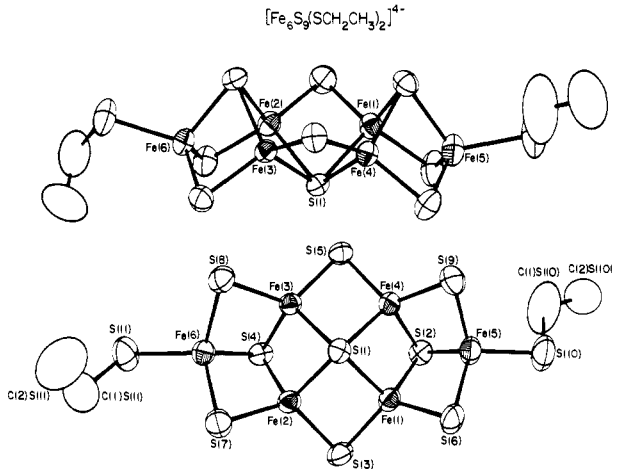

Figure 9. Structure of $[Fe_6S_9(SEt)_2]^{4-}$ as its Et_4N^+ salt, showing the atom labeling scheme and 50% probability ellipsoids. The lower view is down the idealized C_2 axis containing S(1) and perpendicular to the Fe(1–4) plane.

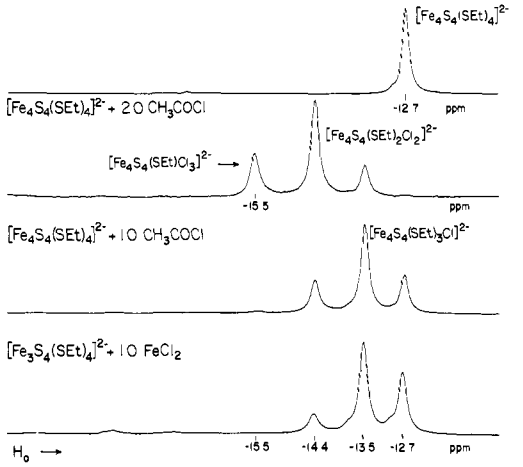

Figure 10. ^1H NMR spectra (300 MHz) demonstrating the $Fe_3S_4 \rightarrow Fe_4S_4$ core conversion reaction in CD_3CN solution. The reaction systems initially contained ~0.10 M cluster salt to which the specified equivalents of solid $FeCl_2$ or acetyl chloride were added. Only the methylene spectral region is shown; signal assignments are indicated.

has not been achieved as yet in Fe–S clusters but is found in $[Co_8S_6(SPh)_8]^{4-}$,[41] recently prepared in this laboratory. The inverse Fe/S site population occurs in $[Fe_6S_8(PEt_3)_6]^{2+}$.[18]

Previously $[Fe_6S_9(S\text{-}t\text{-}Bu)_2]^{4-}$ was synthesized by the reaction of $FeCl_3$, Li_2S, and t-BuSLi in methanol in the presence of excess LiOMe.[13,14] It was isolated in pure crystalline form only as its $Me_3NCH_2Ph^+$ salt, which is nearly insoluble in acetonitrile and only moderately soluble in Me_2SO. The one-step synthesis of $[Fe_6S_9(SEt)_2]^{4-}$ by reaction 11 is equally convenient, and the Et_4N^+ cluster salt is more soluble and easier to work with in different solvents than is $(Me_3NCH_2Ph)_4[Fe_6S_9(S\text{-}t\text{-}Bu)_2]$. This behavior facilitates an examination, currently underway, of the reaction chemistry of $[Fe_6S_9(SR)_2]^{4-}$ clusters.

Reactivity Comparison of $[Fe(SPh)_4]^{2-}$ and $[Fe(SEt)_4]^{2-}$. Reaction 4 afforded $(Et_4N)_2[Fe_2S_2(SPh)_4]$ in 71% yield.[4] When carried out under ambient conditions with 1 equiv of sulfur an 84% in situ yield of this product was obtained.[4] Reaction 7 proceeds rapidly at room temperature and gives an 80% yield. When $(Et_4N)_2[Fe(SPh)_4]$ was refluxed with 1.5 equiv of sulfur in acetone for 24 h, a quantitative yield of sparingly soluble $(Et_4N)_2[Fe_2S_2(SPh)_4]$ was isolated. In contrast, reaction 8 at room temperature gave 66% $(Et_4N)_3[Fe_3S_4(SEt)_4]$, the other product being $[Fe_2S_2(SEt)_4]^{2-}$. A system containing $(Et_4N)_2[Fe(SPh)_4]$ and 1.5 equiv of sulfur in acetonitrile at 80 °C for 48 h afforded the salts of $[Fe_2S_2(SPh)_4]^{2-}$ (~60%) and $[Fe_3S_4(SPh)_4]^{3-}$ (24%). No Fe_6S_9 cluster was detected. This is to be compared with the 71% yield of $(Et_4N)_4[Fe_6S_9(SEt)_2]$ in reaction 11. These observations are sufficient to provide a qualitative demonstration of the enhanced reactivity of $[Fe(SEt)_4]^{2-}$ vs. $[Fe(SPh)_4]^{2-}$, especially in respect of formation of Fe_3S_4 and Fe_6S_9 clusters under comparable conditions. The reaction sequences and mechanisms leading to formation of these clusters are not presently known. However, because all reactions involve the reduction of elemental sulfur to sulfide, it is probable that the much lower (by 0.55 V) redox potential of $[Fe(SEt)_4]^{2-}$ is primarily responsible for the greater reactivity of this complex.

Cluster Conversion Reactions. Several reactions, included in Scheme II (Figure 1) have been accomplished that effect conversion of one type of core structure into another. The observations that follow were made in situ.

(a) $Fe_2S_2 \rightarrow Fe_4S_4$. Reaction 13 was demonstrated by heating a saturated solution of $(Me_3NCH_2Ph)_2[Fe_2S_2(SEt)_4]$ in acetonitrile at 80 °C for 12 h. The ^1H NMR and absorption spectra at the end of this treatment correspond to those of pure $[Fe_4S_4(SEt)_4]^{2-}$ (Figures 2 and 3). No other paramagnetic species was detected in the NMR spectrum. The conversion reaction resulted in ~95% yield of the tetranuclear cluster. Comparable extents of conversion but over much longer periods of time have been found for reaction 5 when conducted at ambient temperature in media containing methanol[4] or water.[42]

(b) $Fe_3S_4 \rightarrow Fe_4S_4$. This conversion was investigated in the form of reaction 14 in acetonitrile at ambient temperature; pertinent NMR spectra are presented in Figure 10. Reaction of $[Fe_3S_4(SEt)_4]^{3-}$ with 1.0 equiv of solid $FeCl_2$ results in elimination of the −33.5 ppm signal of the trinuclear cluster and the appearance of signals at −12.7, −13.5, and −14.4 ppm in the intensity ratio 1:1.9:0.4. The first of these is the CH_2 resonance of $[Fe_4S_4(SEt)_4]^{2-}$. The others were found to be CH_2 resonances of mixed-ligand Fe_4S_4 clusters, examples of which have been shown to be formed in reaction 15.[43] Treatment of $[Fe_4S_4(SEt)_4]^{2-}$ with

$$[Fe_4S_4(SR)_4]^{2-} + n CH_3COCl \rightarrow [Fe_4S_4(SR)_{4-n}Cl_n]^{2-} + n CH_3COSR \quad (15)$$

1.0 equiv of acetyl chloride gives the same three resonances found for the $FeCl_2$ reaction products. Reaction with 2.0 equiv virtually eliminates the $[Fe_4S_4(SEt)_4]^{2-}$ resonance, decreases and increases the −13.5 and −14.4 ppm signals, respectively, and affords a new feature at −15.5 ppm. Although the signal intensities do not adhere closely to a statistical distribution of mixed-ligand species,[44] the pattern of intensity changes is qualitatively consistent with the indicated assignments. On the basis of these assignments ~30% of the Fe_4S_4 products formed from $[Fe_3S_4(SEt)_4]^{3-}$ and $FeCl_2$ is $[Fe_4S_4(SEt)_4]^{2-}$. Product formation must involve a one-electron reduction of the initial cluster (or some fragment thereof) and is represented by reaction 16 for the mixed-ligand (n = 1, 2)

$$[Fe_3S_4(SEt)_4]^{3-} + FeCl_2 \rightarrow [Fe_4S_4(SEt)_{4-n}Cl_n]^{2-} + {}^1/_2EtSSEt + (2-n)Cl^- + (n-1)EtS^- \quad (16)$$

clusters. $[Fe_4S_4(SEt)_4]^{2-}$ cannot be produced directly but can be generated by ligand exchange/substitution reactions involving the n = 1, 2 clusters and EtS^-. When the reaction was carried out on a preparative scale in the presence of 1.2 equiv of NaSEt, a 63% purified yield of n-Bu_4N^+ salt of the cluster was obtained. In this case core conversion is simply represented by reaction 17.

$$[Fe_3S_4(SEt)_4]^{3-} + FeCl_2 + NaSEt \rightarrow [Fe_4S_4(SEt)_4]^{2-} + {}^1/_2EtSSEt + NaCl + Cl^- \quad (17)$$

(41) Hagen, K. S.; Christou, G.; Holm, R. H. *J. Am. Chem. Soc.* **1982**, *104*, 1744.

(42) Cambray, J.; Lane, R. W.; Wedd, A. G.; Johnson, R. W.; Holm, R. H. *Inorg. Chem.* **1977**, *16*, 2565.

(43) Johnson, R. W.; Holm, R. H. *J. Am. Chem. Soc.* **1978**, *100*, 5338.

(44) In these systems small amounts of black precipitate formed and may contribute to the departure from statistical behavior. No precipitate was observed in the $[Fe_3S_4(SEt)_4]^{3-}/FeCl_2$ system.

The trinuclear → tetranuclear core conversion demonstrated is the first example of this process for synthetic Fe–S clusters. In terms of the initial trinuclear structure this process apparently is not the same as the $Fe_3S_x \rightarrow Fe_4S_4$ reactions noted at the outset for aconitase[10] and *D. gigas* ferredoxin II.[11,12] In the oxidized (3Fe(III)) state these proteins are characterized by an EPR signal at $g \cong 2.01$.[11,12,46] This signal is found for all known oxidized Fe_3S_x sites even though there are apparent structural differences.[8,9] The recent EXAFS analysis of *D. gigas* ferredoxin II leads to the possibility of a site configuration with two Fe–Fe separations of ~2.7 Å,[9] in marked contrast to the cyclic structure of *A. vinelandii* ferredoxin I, with Fe–Fe distances of ~4.1 Å.[8] The EPR spectrum of $[Fe_3S_4(SEt)_4]^{3-}$ ($g = 4.2$) is inconsistent with the electronic structures of the protein sites, indicating a different type of trinuclear arrangement. The reverse reaction, $Fe_4S_4 \rightarrow Fe_3S_x$, has been demonstrated with several proteins under reducing[12] and oxidizing[47-49] conditions. We have not observed a corresponding reaction with synthetic clusters. Conversion reactions involving Fe_4S_4 clusters are currently limited to reactions 5, 13, and 14, $[Fe_2S_2(SR)_4]^{3-} \rightarrow [Fe_4S_4(SR)_4]^{2-}$[42] and $[Fe_4S_4Cl_4]^{2-} \rightarrow [Fe_2S_2Cl_4]^{2-}$, the last being carried out under oxidizing conditions.[45]

Summary. This research has demonstrated the occurrence of all reactions in Scheme II, leading to the synthesis of Fe_2S_2, Fe_3S_4, Fe_4S_4, and Fe_6S_9 clusters from the readily accessible (but extremely oxidatively sensitive) mononuclear complex $[Fe(SEt)_4]^{2-}$. Also provided are the detailed structures of examples of the two newest types of Fe–S–SR clusters, $[Fe_3S_4(SR)_4]^{3-}$ and $[Fe_6S_9(SR)_2]^{4-}$. Judging from the time dependence of signal intensities in Figure 4, the initial sequence of events in cluster formation is $[Fe(SEt)_4]^{2-} \rightarrow [Fe_2S_2(SEt)_4]^{2-} \rightarrow [Fe_3S_4(SEt)_4]^{3-}$. Roughly coincident with the formation of trinuclear cluster is the appearance of a paramagnetic species with a signal at −8.3 ppm. Inasmuch as the intensity of this signal decays as $[Fe_4S_4(SEt)_4]^{2-}$ and $[Fe_6S_9(SEt)_2]^{4-}$ are produced at 80 °C, this species lies on the reaction pathway to one or both clusters. Given the independent occurrence of reaction 13, our present hypothesis is that the −8.3 ppm species is a product of $[Fe_3S_4(SEt)_4]^{3-}$ and is a precursor to $[Fe_6S_9(SEt)_2]^{4-}$. Attempts to isolate and characterize this species are in progress. Finally, because the actual reaction sequences leading to cluster formation in the overall reactions 8, 10, and 11 are unknown, we have refrained from expressing these reactions in any stoichiometric form. Limiting stoichiometries for the other reactions of Scheme II are obvious, and these and related expressions have been presented elsewhere in connection with the derivation of Scheme I.[4]

Acknowledgment. This research has been supported by NIH Grant GM-28856. NMR and X-ray equipment used in this research was obtained by NSF Grants CHE 80-00670 and CHE 80-08891.

Registry No. $(Et_4N)_2[Fe(SEt)_4]$, 82661-04-9; $(Me_3NCH_2Ph)_2[Fe(SEt)_4]$, 85585-64-4; $(Et_4N)_2[Fe(SPh)_4]$, 77403-03-3; $(Me_3NCH_2Ph)_2[Fe_2S_2(SEt)_4]$, 85647-21-8; $(Et_4N)_3[Fe_3S_4(SEt)_4]$, 85647-20-7; $(Et_4N)_3[Fe_3S_4(SPh)_4]$, 82661-12-9; $(Et_4N)_4[Fe_6S_9(SEt)_2]$, 85585-66-6; $(Et_4N)_4[Fe_6S_9(SEt)_2]\cdot 4MeCN$, 85585-67-7; $(n\text{-}Bu_4N)_2[Fe_4S_4(SEt)_4]$, 53433-48-0; $(Et_4N)_2[FeCl_4]$, 15050-84-7.

Supplementary Material Available: Thermal and cation positional parameters, calculated hydrogen atom positions, and values of $10|F_o|$ and $10|F_c|$ for $(Et_4N)_3[Fe_3S_4(SPh)_4]$; thermal parameters, cation and solvate molecule positional parameters, calculated hydrogen atom positions, and values of $10|F_o|$ and $10|F_c|$ for $(Et_4N)_4[Fe_6S_9(SEt)_2]\cdot 4MeCN$ (80 pages). Ordering information is given on any current masthead page.

(45) Wong, G. B.; Bobrik, M. A.; Holm, R. H. *Inorg. Chem.* **1978**, *17*, 578.
(46) Ruzicka, F. J.; Beinert, H. *J. Biol. Chem.* **1978**, *253*, 2514.
(47) Thomson, A. J.; Robinson, A. E.; Johnson, M. K.; Cammack, R.; Rao, K. K.; Hall, D. O. *Biochim. Biophys. Acta* **1981**, *627*, 423.
(48) Johnson, M. K.; Spiro, T. G.; Mortenson, L. E. *J. Biol. Chem.* **1982**, *257*, 2447.
(49) Bell, S. H.; Dickson, D. P. E.; Johnson, C. E.; Cammack, R.; Hall, D. O.; Rao, K. K. *FEBS Lett.* **1982**, *142*, 143.

Mechanistic Aspects of a Homogeneous Carbon Monoxide Hydrogenation Catalyst—$Ir_4(CO)_{12}$ in Molten $AlCl_3$–NaCl

James P. Collman,* John I. Brauman, Gerald Tustin, and Grady S. Wann III

Contribution from the Department of Chemistry, Stanford University, Stanford, California 94305. *Received October 22, 1982*

Abstract: The "homogeneous Fischer–Tropsch catalysis" first described by Muetterties et al. was kinetically examined in both a single-pass flow reactor and a continuous recycle apparatus. In our hands the $Ir_4(CO)_{12}$ precatalyst in molten aluminum chloride–sodium chloride (2:1) at 175 °C and 1 atm of hydrogen and carbon monoxide (3:1) produces methane, ethane, and chloromethane as the major carbon-containing products. In addition, a stoichiometric amount of methane is formed when the $Ir_4(CO)_{12}$ is introduced into the molten $AlCl_3$–NaCl at the onset of catalysis. Flow rate studies and the effect of added chloromethane on the active catalytic system implicate chloromethane (or methanol) as a primary reaction intemediate. Heterogeneous iridium-on-alumina catalysts show different behavior under these reaction conditions, whereas a mononuclear precatalyst, $IrCl(CO)_3$, shows similar chemistry. From the experimental evidence presented here, we conclude that this reaction involves the homogeneous reduction of CO to chloromethane, followed by homologation and/or hydrogenation reactions leading to the hydrocarbon products. Because these results differ significantly from those reported earlier, we conclude that this system must involve a different active catalyst.

Intense interest in new technology to supplement a dwindling petroleum supply has fostered renewed activity in Fischer–Tropsch chemistry. Along with advances in traditional heterogeneous catalysis[2,3] (especially with regard to reaction mechanism),[4,5] homogeneous carbon monoxide reduction has been a subject of active study during the past decade.[6,7] With the potential to offer increased selectivity to desired products, more control at the catalytic site, and greater tolerance to poisoning from sulfur-

(1) Abstracted from the Ph.D. thesis of Grady S. Wann III, Stanford University, 1982.
(2) Vannice, M. A. *Catal. Rev.—Sci. Eng.* **1976**, *14*, 153–191 and references therein.
(3) Frohning, C. D. In "New Syntheses with Carbon Monoxide"; Falbe, J., Ed.; Springer-Verlag: New York, 1980; pp 309–371, and references therein.
(4) Biloen, P.; Sachtler, W. *Adv. Catal.* **1981**, *30*, 165–216 and references therein.
(5) Rofer-DePoorter, C. K. *Chem. Rev.* **1981**, *81*, 447–474 and references therein.
(6) Masters, C. *Adv. Organomet. Chem.* **1979**, *17*, 61–103.
(7) Muetterties, E. L.; Stein, J. *Chem. Rev.* **1979**, *79*, 479–490.

0002-7863/83/1505-3913$01.50/0